Electronic supplementary information

Strategies for Deposition of $LaFeO_3$ Photocathodes: Improving Photocurrent with a Polymer Template

Emma Freeman,[1,2] Santosh Kumar,[1,3] Veronica Celorrio,[4] Min Su Park,[5] Jong Hak Kim,[5] David J. Fermin[2] and Salvador Eslava[1,3*]

1. Department of Chemical Engineering, University of Bath, Bath, BA2 7AY, UK

2. School of Chemistry, University of Bristol, Cantock's Close, Bristol, BS8 1TS, UK

3. Department of Chemical Engineering, Imperial College London, SW7 2AZ London, UK

4. Diamond Light Source Ltd., Diamond House, Harwell Campus, Didcot, OX11 0DE, UK.

5. Department of Chemical and Biomolecular Engineering, Yonsei University, Seoul 03722, South Korea

* s.eslava@imperial.ac.uk

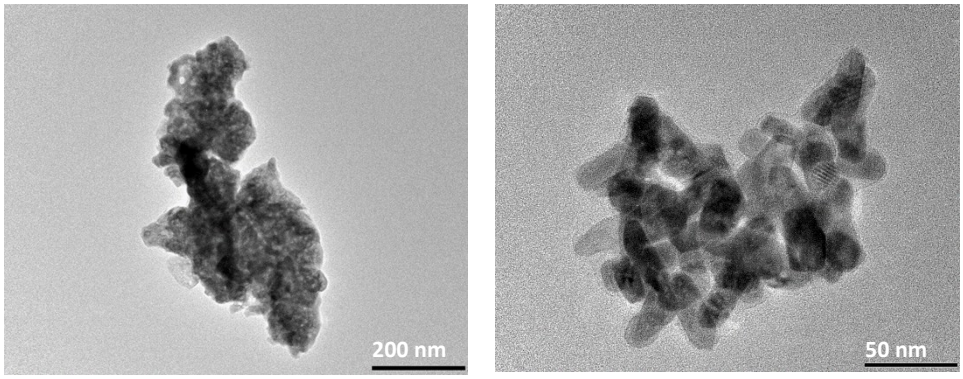

Figure S1: HR-TEM images of LFO powders calcined at 600°C for 4 h.

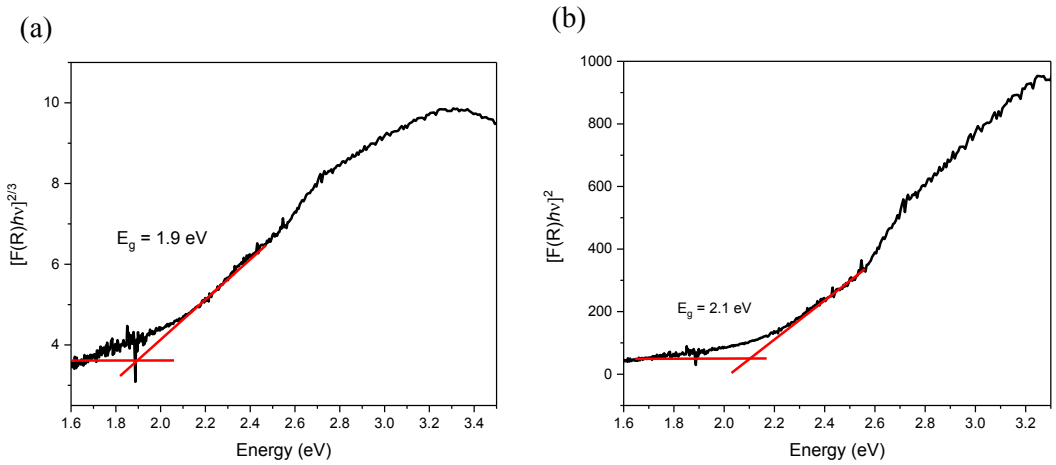

Figure S2: Tauc plot of LFO powder calcined at 600°C, for (a) a direct forbidden optical transition (n=3/2) or (b) a direct allowed transition (n=1/2).[1,2] Optical transitions in these complex and polycrystalline ferrite, featuring elemental disorder and band tailing, could significantly deviate from standard direct transitions, hence we considered both allowed and forbidden transitions to determine the band gap to be in the range of 1.9-2.1 eV.

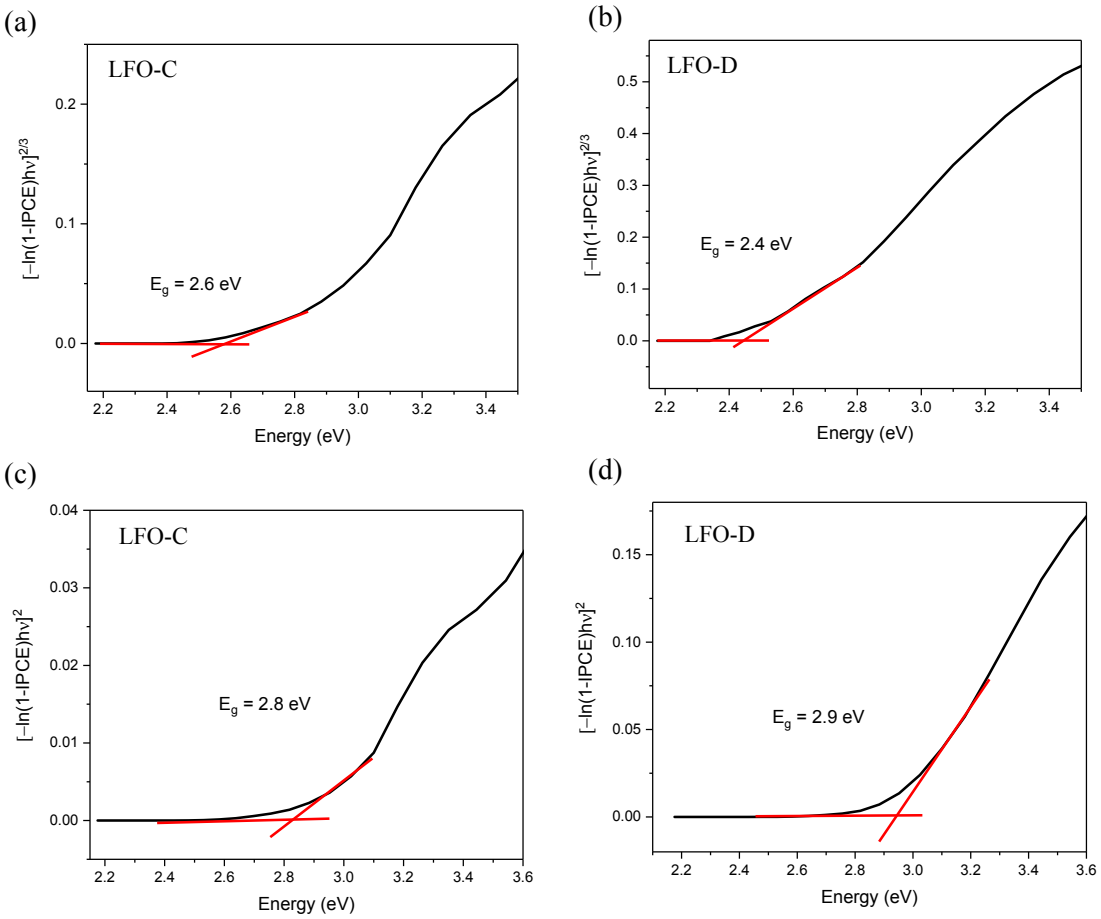

Figure S3: Tauc plots employing IPCE for (a,c) LFO-C and (b,d) LFO-D to determine band gap using (a,b) a direct forbidden optical transition (n=3/2) or (c,d) a direct allowed transition (n=1/2). [2,3] Optical transitions in these complex and porous polycrystalline ferrite films, featuring elemental disorder and band tailing, could significantly deviate from standard direct transitions, hence we considered both allowed and forbidden direct transitions to determine the band gap to be in the range of 2.4-2.9 eV.

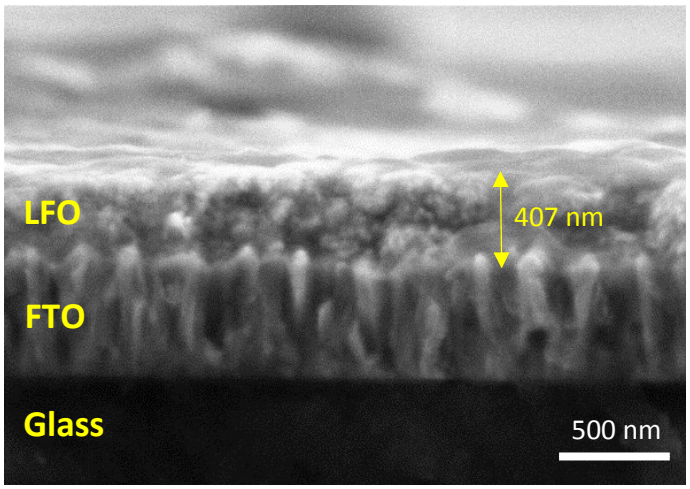

Figure S4: Cross-section FE-SEM of LFO-D (3 layers) to determine film thickness.

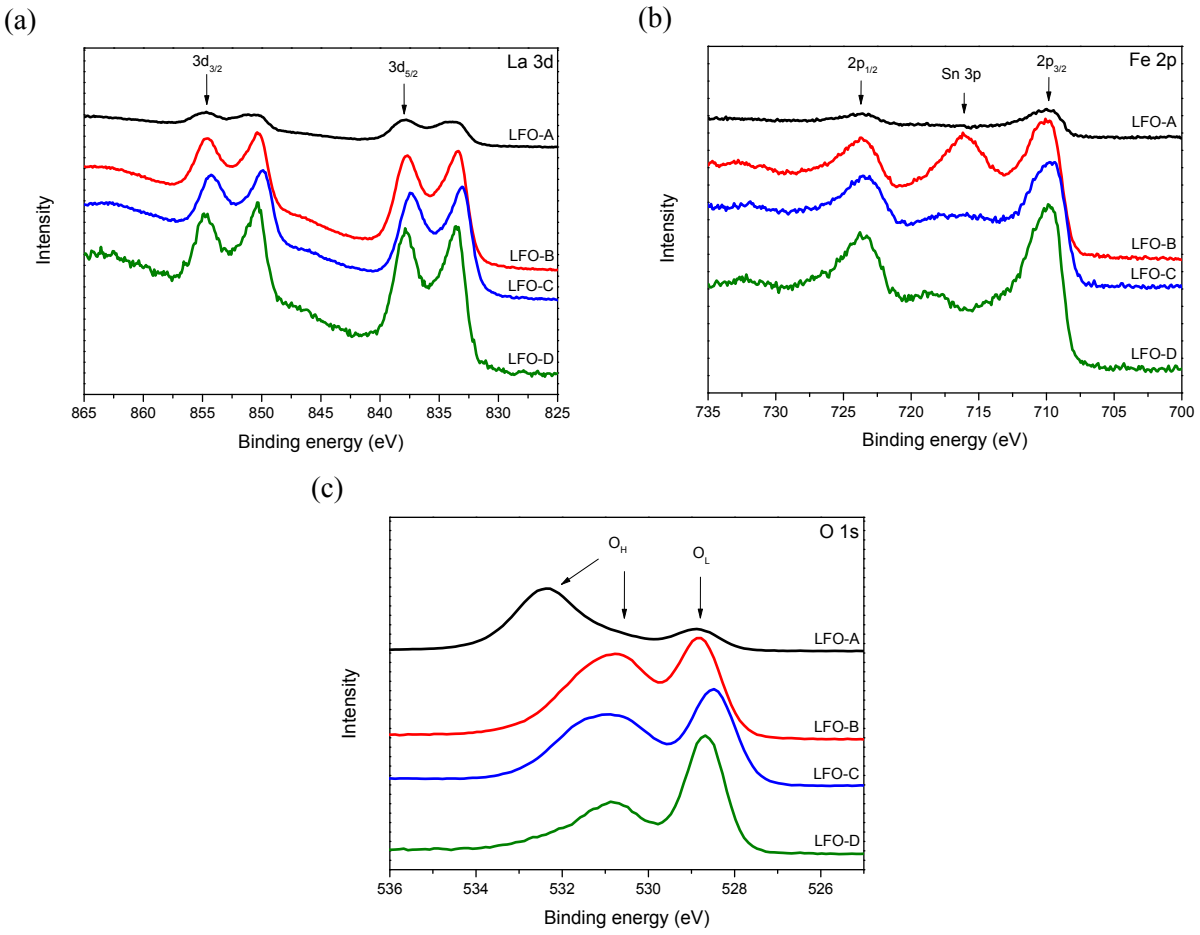

Figure S5: (a) XPS spectra of La 3d, (b) Fe 2p and (c) O 1s for films LFO-A, B, C and D.

Sample	La	Fe

LFO-A	1	0.8
LFO-B	1	1.1
LFO-C	1	1
LFO-D	1	0.8

Table S1: Quantification of La:Fe ratios for prepared LFO films from XPS survey spectra using CasaXPS fitting software.

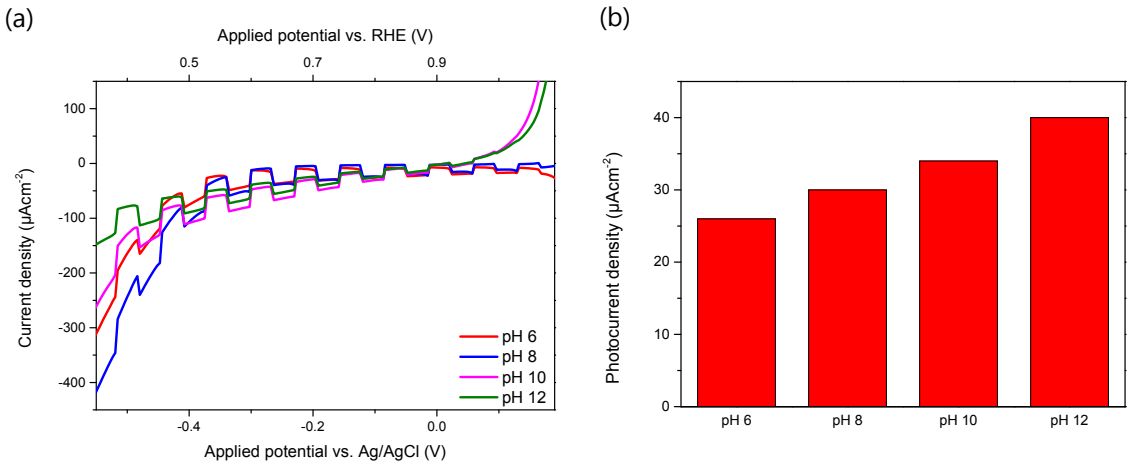

Figure S6: (a) Photocurrent measurements of a LFO film with 0.1 M Na_2SO_4 at pH 6, 8 and 10 (pH increased with NaOH) and (b) measured maximum photocurrent achieved from electrolytes of pH 6-12 at various potentials.

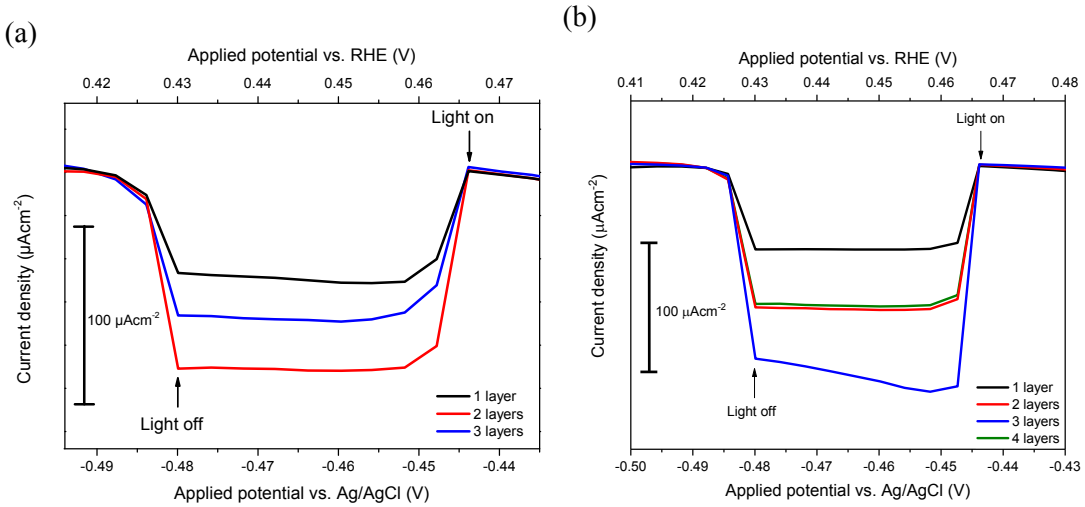

Figure S7: (a) Normalized photocurrent measurements at point of interest for LFO-C with the application of 1-3 LFO layers for optimization and (b) normalized photocurrent measurements for LFO-D with the application of 1-4 LFO layers for optimization.

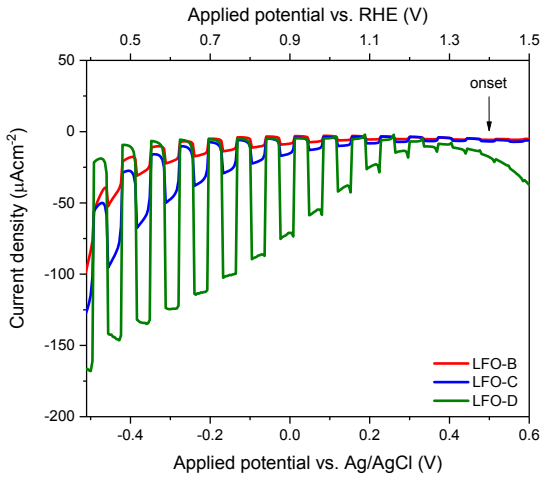

Figure S8: LSV measurements from +0.6 to -0.5 V_{AgCl} for LFO-B, -C and -D under chopped solar illumination with a 0.1 M Na_2SO_4 pH 12 electrolyte, to determine onset potential.

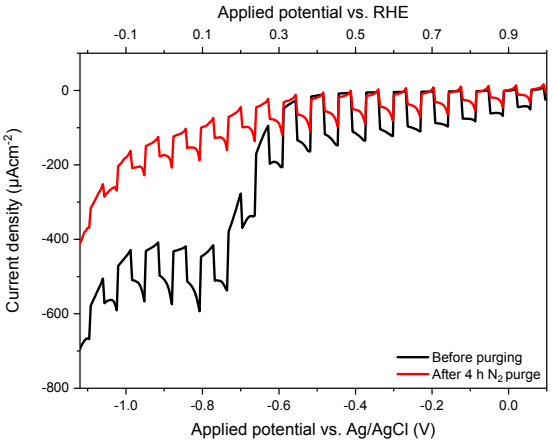

Figure S9: LSV measurements from +0.1 to -1.12 V_{AgCl} for LFO-D under chopped solar illumination with a 0.1 M Na_2SO_4 pH 12 electrolyte, in an unpurged (O_2 present) and a N_2 purged system (purged for 4 hours).

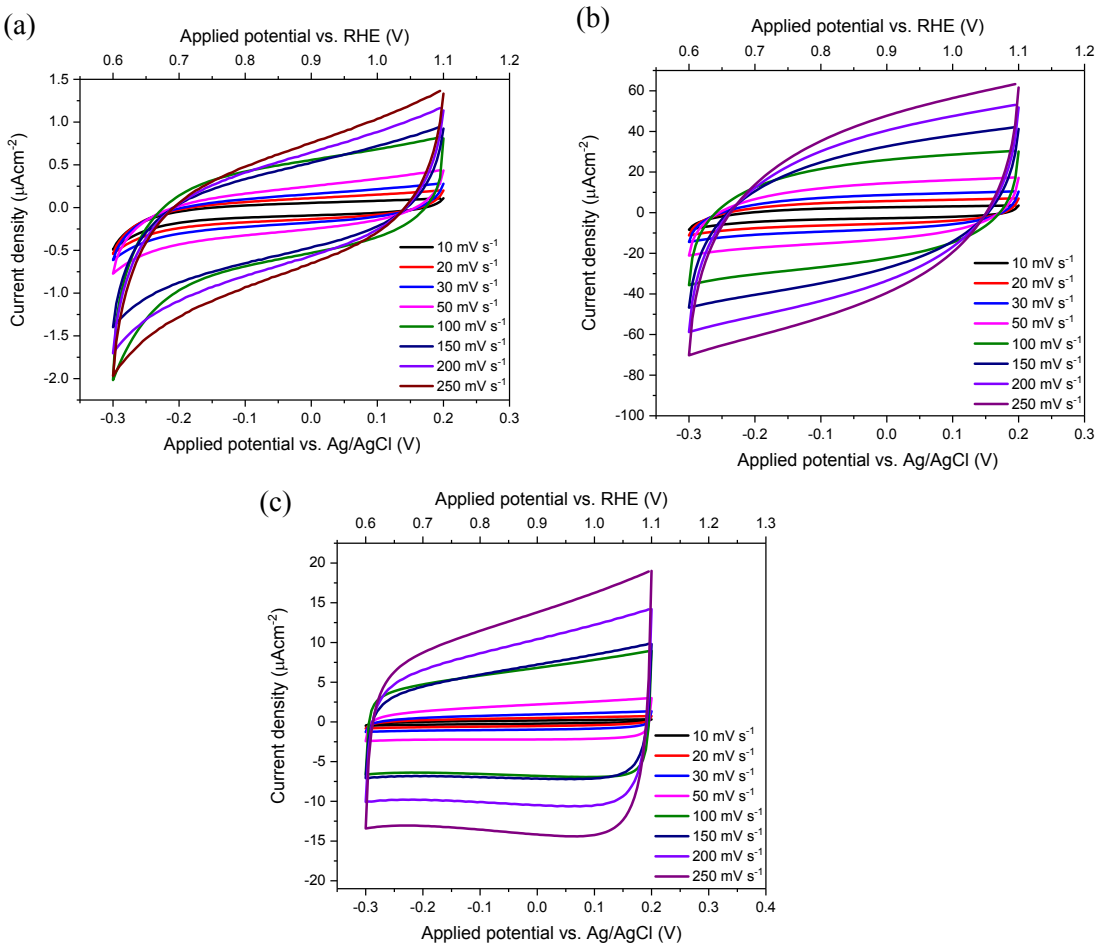

Figure S10: Cyclic voltammetry curves at scan rates between 10 and 250 mV s^{-1} for (a) LFO-B, (b) LFO-C and (c) LFO-D.

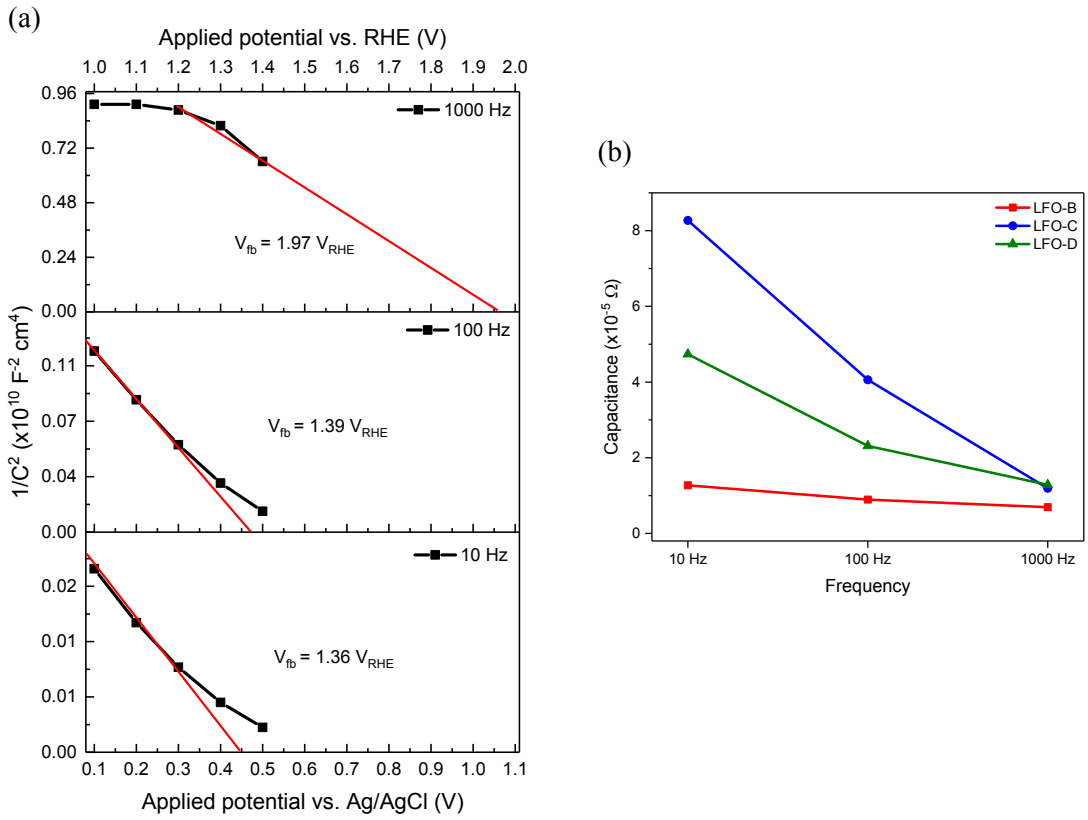

Figure S11: (a) Example Mott-Shottky plots for LFO-D at different frequencies and (b) capacitance values determined from EIS measurements as a function of frequency, measured at -0.3 V_{AgCl}. Results show frequency dispersion due to the nanostructured porous nature of the films. In this situation, simple models applied for Mott-Shottky analysis are not suitable. Further elaboration on this topic can be found elsewhere.[4]

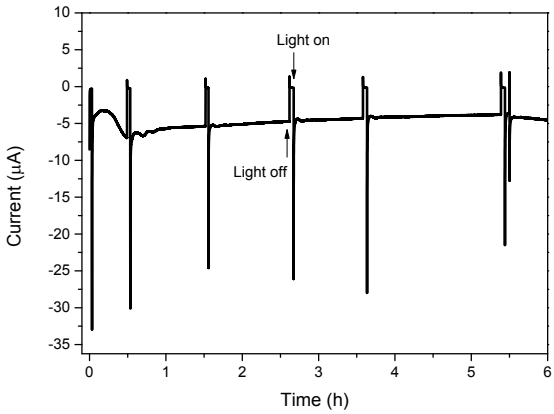

Figure S12: Current data from H_2 evolution measurement at a potential of +0.43 V_{RHE} under constant solar illumination (100 mW cm^{-2}).

1 R. López and R. Gómez, *J. Sol-Gel Sci. Technol.*, 2012, **61**, 1–7.

2 M. Scafetta, A. Cordi, J. Rondinelli and S. May, *J. Phys. Condens. Matter*, 2014, **26**, 505502.

3 T. M. Ng, M. T. Weller, G. P. Kissling, L. M. Peter, P. Dale, F. Babbe, J. De Wild, B. Wenger, H. J. Snaith and D. Lane, *J. Mater. Chem. A*, 2017, **5**, 1192–1200.

4 A. Hankin, F. E. Bedoya-Lora, J. C. Alexander, A. Regoutz and G. H. Kelsall, *J. Mater. Chem. A*, 2019, Advance Article. DOI: 10.1039/C9TA09569A.